JOURNAL OF GEOPHYSICAL RESEARCH, VOL. 106, NO. D13, PAGES 14,313-14,325, JULY 16, 2001

Seasonal variation of water vapor in the lower stratosphere observed in Halogen Occultation Experiment data

William J. Randel,[1] Fei Wu,[1] Andrew Gettelman,[1] J. M. Russell III,[2]
Joseph M. Zawodny,[3] and Samuel J. Oltmans[4]

Abstract. The seasonal cycle of water vapor in the lower stratosphere is studied based on Halogen Occultation Experiment (HALOE) satellite observations spanning 1991-2000. The seasonal cycle highlights fast, quasi-horizontal transport between tropics and midlatitudes in the lowermost stratosphere (near isentropic levels ~380-420 K), in addition to vertical propagation above the equator (the tropical "tape recorder"). The rapid isentropic transport out of the tropics produces a layer of relatively dry air over most of the globe throughout the year, and the seasonal cycle in midlatitudes of both hemispheres (and over the Arctic pole) follows that in the tropics. Additionally, the Northern Hemisphere summer monsoon has a dominant influence on hemispheric-scale constituent transport. Longitudinal structures in tropical water vapor and ozone identify regions of strong coupling to the troposphere; an intriguing result is that the solstice minima in water vapor and ozone are spatial separated from maximum convection and coldest tropical temperatures. Detailed comparisons with tropical aircraft measurements and the long record of balloon data from Boulder, Colorado, demonstrate the overall high quality of HALOE water vapor data.

1. Introduction

Water vapor provides a valuable tracer for studying transport into and within the stratosphere The extreme dryness of the stratosphere was used by *Brewer* [1949] to deduce that air entered the stratosphere primarily in the tropics The seasonal variation of water vapor in the tropical lower stratosphere is clearly tied to seasonality in tropical tropopause temperatures [*Mote et al* , 1996], and the vertical propagation of this seasonal cycle in the tropics provides information on the mean upward (Brewer-Dobson) circulation [*Hall and Waugh*, 1997; *Mote et al.*, 1998; *Andrews et al* , 1999; *Michelson et al* , 2000]. Observations of water vapor in the midlatitude lower stratosphere also show an annual cycle that is temporally linked with the tropics [*Mastenbrook*, 1974; *Hyson*, 1983; *Mastenbrook and Oltmans*, 1983, *McCormick et al* , 1993, *Hintsa et al.*, 1994, *Boering et al.*, 1995]. The inference from these analyses is that rapid transport occurs between the tropics and midlatitudes in the lower stratosphere; this conclusion is reinforced by observations of radioactive isotopes following tropical bomb explosions [*Feely and Spar*, 1960; *Newell*, 1963], volcanic aerosols after tropical eruptions [*Trepte et al.*, 1993], and the seasonal cycle of CO_2 [*Boering et al.*, 1995; *Strahan et al.*, 1998]. This region of fast transport is most evident for altitudes between the tropopause and ~20 km; above 20 km the tropics appear more isolated from midlatitudes This distinct behavior has prompted several names for this region of the lower stratosphere: *Trepte and Hitchman* [1992] and *Hitchman et al.* [1994] refer to it as the "lower transport regime" (as opposed to the "upper transport regime" above ~20 km), and *Rosenlof et al.* [1997] coined the term "tropically controlled transition region "

The Halogen Occultation Experiment (HALOE) has made high-quality, global measurements of stratospheric water vapor since late 1991 These measurements have relatively high vertical resolution (~2 km), which can resolve the global structure of water vapor from the tropopause into the mesosphere [*Russell et al* , 1993]. These data have been used by *Tuck et al* [1993], *Rosenlof et al.* [1997], *Randel et al* [1998], and *Jackson et al.* [1998] to study the global seasonal cycle of stratospheric water vapor and connections between tropics and midlatitudes This paper presents an updated estimate of the seasonal cycle in HALOE data, with particular emphasis on the details of transport between tropics and midlatitudes in the lowermost stratosphere While the concept of fast transport in this region of the atmosphere is not novel, the HALOE water vapor data provide a particularly clear depiction of this fundamental process These data furthermore highlight the dominant role of the Northern Hemisphere (NH) summer monsoon circulations for influencing transport and tropospheric coupling on a hemispheric scale and suggest very weak transport in the summer polar lower stratosphere. We also briefly discuss climatological longitudinal structures evident in the lower stratospheric HALOE data and show correlated behavior in lower stratospheric ozone measurements. The seasonal variability in HALOE measurements are compared in detail with available tropical aircraft measurements and also with the long record of balloon measurements at Boulder, Colorado Although some limitations of HALOE water vapor are evident just above the tropical tropopause, overall these comparisons demonstrate that HALOE accurately captures the global seasonal cycle.

[1]National Center for Atmospheric Research, Boulder, Colorado
[2]Center for Atmospheric Sciences, Hampton University, Hampton, Virginia
[3]NASA Langley Research Center, Langley Park, Maryland
[4]NOAA Climate Monitoring and Diagnostics Laboratory, Boulder, Colorado

Paper number 2001JD900048
0148-0227/01/2001JD900048$09 00

2. Data and Analyses

2.1. HALOE Water Vapor

The HALOE instrument provides high-quality, vertical profiles of water vapor, derived from solar occultation measurements, as discussed by *Russell et al.* [1993] and *Harries et al.* [1996]. We use the V19 retrieval product obtained in so-called level 2 format. The vertical resolution of the HALOE measurements is ~2 km, but the level 2 data used here are slightly oversampled with a ~1.3-km vertical spacing (12 standard levels per decade of pressure). The HALOE measurements extend down to the approximate local tropopause level, below which cloud effects contaminate a significant fraction of the retrievals.

Extensive comparisons of HALOE data with other stratospheric water vapor measurements have been conducted in the Stratospheric Processes and Their Role in Climate (SPARC) water vapor assessment study [*World Meteorological Organization (WMO)*, 2000]. Briefly, HALOE shows a slight dry bias in the lower stratosphere (60-100 mbar) by ~5-20% compared to available aircraft or balloon measurements. This bias in the lower stratosphere is partly due to errors in the temperature-dependent O_2 continuum absorption used in the V19 HALOE retrieval, which will be improved in the next data release. An additional factor is that the ~2-km vertical resolution of HALOE may underestimate the magnitude of seasonal extrema in the tropics, where the vertical separation between maxima and minima for the tape recorder signal is ~3 km [*Mote et al.*, 1996, their Figure 1]. Our comparisons with balloon measurements in Boulder (below) suggest that this problem is less important in midlatitudes.

The HALOE solar occultation technique provides 15 sunrise and 15 sunset measurements per day, with each sunrise or sunset group near the same latitude but spaced ~24° apart in longitude. The latitudinal sampling progresses in time, so that much of the latitude range 60°N-60°S is sampled in 1 month; the measurements extend to polar regions during spring through late summer. Our analyses here focus on the seasonal variation of zonal means and also on longitudinal structures (which are of interest in themselves and also necessary for comparisons with the Boulder balloon data). For the "zonal mean" analyses the profile measurements are binned into monthly samples according to analyzed potential vorticity (PV) fields, expressed in terms of equivalent latitude [*Randel et al.*, 1998]. This has the dual advantage of separating physically distinct air masses (inside versus outside of the stratospheric polar vortex) and extending the effective latitude range of the data; the results are nearly identical to direct longitudinal means outside of high latitudes. The seasonal cycle is derived from a harmonic regression analysis of the combined sunrise plus sunset measurements sampled monthly on a 4° latitude grid, including annual and semiannual harmonics. The time period included is January 1992 to December 1999.

Longitudinal variations of the seasonal cycle are derived by temporal harmonic analysis of monthly data binned on latitude-longitude grids (with a 4° × 30° latitude-longitude resolution). The monthly binning is performed using a Gaussian spatial weighting, with half widths of 1° in latitude and 10° in longitude. This combination of space-time analysis produces reasonably detailed but smooth longitudinal information from the HALOE sampling.

Because HALOE measurements do not cover polar regions for much of the year, we extend our water vapor analyses to include polar data from the Microwave Limb Sounder (MLS) prototype V104 retrieval [*Pumphrey*, 1999]. These data cover 20 months (September 1991 to April 1993) and provide polar measurements during (approximately) alternate months. These data have vertical resolution of ~2.5 km (twice the HALOE sampling interval used here), with retrievals on pressure levels spanning 100-0.1 mbar. We construct a seasonal cycle from the MLS data in an identical manner to our HALOE data treatment (with the harmonic analysis providing smooth interpolation of individual months with missing data) and then use the MLS results to fill polar regions not observed by HALOE. Small adjustments (constant offsets of a few percent) are made to the MLS data to join smoothly with the highest-latitude HALOE data each month. This produces a continuous global seasonal cycle at and above 100 mbar; between the tropopause and 100 mbar only HALOE data are available, and polar regions are left blank in the plots when data are missing.

2.2 Aircraft and Balloon Water Vapor Measurements

There are relatively few data sets that can quantify the seasonal cycle of water vapor above the tropical tropopause. Probably the best in situ data for such analyses are aircraft measurements from several campaigns during 1994-1997 (Airborne Southern Hemisphere Ozone Experiment (ASHOE), Stratospheric Tracers of Atmospheric Transport (STRAT), and Photochemistry of Ozone Loss in the Arctic Region in Summer (POLARIS)), which provide data over altitudes ~17-21 km for seven individual months These include measurements from March and October 1994 (ASHOE) from the National Oceanic and Atmospheric Administration (NOAA) Aeronomy Laboratory water vapor instrument [*Kley et al.*, 1983], plus data during November 1995; February, August, and December 1996 (STRAT); and September 1997 (POLARIS) from the Harvard University instrument [*Weinstock et al.*, 1994; *Hintsa et al.*, 1999]. The measurement technique for both instruments is based on Lyman fluorescence. The tropical measurements during each of these campaigns come from flights which begin or end in Hawaii, and the spatial sampling is limited to the tropical central Pacific region. According to the *WMO* [2000] comparisons, the HALOE data have a mean bias of ~ -8% with respect to the NOAA data and a ~ -20% bias with respect to the Harvard data. Although there is substantial sampling uncertainty associated with aircraft measurements taken in isolated longitude regions over several years, these are the only in situ measurements available to compare seasonality in this remote region of the atmosphere.

We furthermore include comparisons with the tropical water vapor seasonal cycle derived by *Andrews et al.* [1999], based on empirically derived stratospheric age spectra (estimated from CO_2 observations) coupled with an average near-tropopause water vapor boundary condition derived from radiosonde data during 1993-1997 (as in the work by *Dessler* [1998]). These empirical results provide a continuous estimate of the seasonal cycle in the tropical lower stratosphere, which are in reasonable agreement with the aircraft profile data [see *Andrews et al.*, 1999].

We also compare the HALOE climatology with the water vapor seasonal cycle measured at Boulder, Colorado, by balloon-borne frost point hygrometer instruments [*Oltmans et al.*, 2000; *WMO*, 2000]. These data cover an altitude range up to ~30 km with a vertical resolution of ~0.2 km. The average seasonal cycle is derived from data taken during 1981-1999 using a harmonic analysis, identical to the HALOE fit. The *WMO* [2000] comparisons suggest the HALOE data have a mean bias with respect to these balloon measurements of ~ -5% over 20-30 km and ~ -12% below 20 km.

2.3. SAGE Ozone

Ozone is long-lived in the lower stratosphere and provides another tracer of transport behavior and connection with the (ozone poor) troposphere. We include here some analyses of ozone based on Stratospheric Aerosol and Gas Experiment (SAGE II) measurements [*McCormick et al.*, 1989]. SAGE II is an occultation instrument with similar space-time sampling to HALOE, and our analyses are identical to that discussed above. While HALOE also provides ozone retrievals, the advantage of SAGE II is that the vertical resolution is ~0.5-1 km, substantially better than the 2 km of HALOE. Analyses of HALOE ozone data show similar patterns to SAGE II, but the localized features are more distinct in SAGE (probably because of the increased vertical resolution). We use the version 6.0 retrieval of SAGE II data, covering the period November 1984 to December 1999 (excluding 2 years following the Mount Pinatubo eruption in June 1991).

3. Results

3.1. Seasonal Variation in Lower Stratosphere

Cross sections of water vapor mixing ratio for each month are shown in Plate 1. Each plot includes solid lines denoting isentropic levels of 380, 400, 500 and 600 K, together with a dashed line identifying the tropopause (derived from National Center for Environmental Prediction (NCEP) reanalyses [*Kalnay et al.*, 1996]). Water vapor in the tropical tropopause region begins to decrease in December, with the lowest values centered somewhat north of the equator during January-February. This asymmetric pattern with respect to the equator is also found in SAGE II [*Chiou et al.*, 1997] and MLS [*Pumphrey et al.*, 2000] satellite water vapor measurements. The meridional scale of the tropical minimum in the lowest stratosphere expands rapidly between approximately January and March, so that by March there is a thin layer of dry air covering most of the globe in the lower stratosphere The minimum contours slope downward and poleward, closely following the ~380-400 K isentropic layer; this strongly suggests that the latitudinal movement is due to isentropic transport over this layer. There are stronger meridional gradients in the subtropics of each hemisphere above ~20 km (~500 K), demonstrating more isolation of the tropics above this level. This behavior is consistent with results derived from other measurements, such as the volcanic aerosols of *Trepte et al.* [1993].

During most months a secondary minimum is observed in the tropics above ~20 km, associated with vertical propagation of the annual cycle near the tropopause (the tape recorder of *Mote et al.* [1996]). Figure 1 shows the signature of the tape recorder derived from our seasonal cycle analysis. The minimum near the tropopause occurs in February-April at the equator (but ~2 months earlier at ~15°N; see Plate 1) and can be traced clearly upward to ~28 km. The minimum values show strong attenuation with height in the lowest few kilometers above the tropopause, while the seasonal maximum (unshaded regions in Figure 1) shows less change with height. It is likely that HALOE underestimates the magnitude of the seasonal maximum in the region near the tropopause (100 and 82 mbar), as shown in the aircraft measurement comparisons below.

There are also very low values of water vapor associated with dehydration inside the Antarctic polar vortex evident in Plate 1.

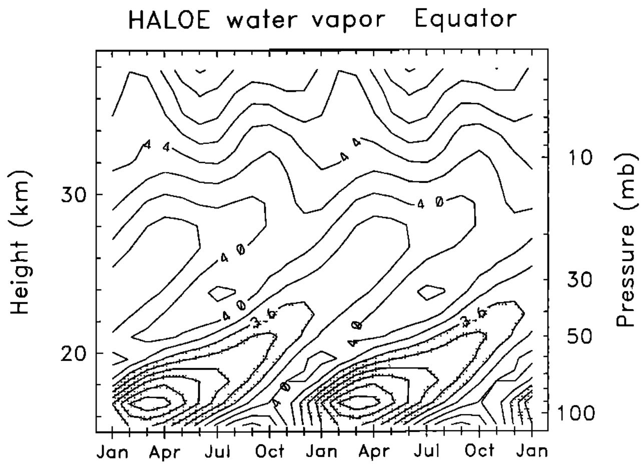

Figure 1. Height-time seasonal variation of water vapor mixing ratio (ppmv) at the equator derived from HALOE data Two consecutive seasonal cycles are shown.

The dehydrated air is seen beginning in July-August at altitudes over ~16-24 km (this is based on MLS data, as HALOE does not observe inside the vortex until September). The patterns of dehydrated vortex air descend in time during August-December, but for the most part remain confined poleward of ~60° equivalent latitude (consistent with the analyses of *Pierce et al.* [1994], and *Rosenlof et al.* [1997]). A remnant of the vortex air is evident in the Antarctic lowermost stratosphere (between the tropopause and ~400 K) at least through January in Plate 1, well after breakup of the polar vortex in late November or December. By February the transport of dry air from the tropics covers most of the Southern Hemisphere (SH), and the Antarctic minimum is no longer distinct. A qualitatively similar polar minimum is found in the Arctic lower stratosphere over ~13-16 km during summer (June-September); this minimum is a result of transport from the tropics, because strong dehydration is not observed inside the vortex during NH winter. The persistence of these minima for several months argues for substantial isolation of and weak transport through the polar lowermost stratosphere during summer.

The seasonal variation of water vapor is furthermore demonstrated by contrasting the January and July data, plotted in isentropic coordinates in Figure 2. This highlights the diabatic ascent of the tropical minimum and cross-isentropic transport of water vapor into the lower stratosphere near 30°-40°N due to the NH summer monsoon circulations (as discussed by *Jackson et al.* [1998]). Note that water vapor in the "middle world" (below 380 K but above the tropopause in extratropics) is substantially higher in the summer hemisphere in both January and July in Figure 2, consistent with SAGE, MLS, and ER 2 measurements [*Pan et al.*, 1997, 2000]. This asymmetry is evidence of enhanced cross-tropopause exchange in the summer hemisphere extratropics, as simulated by *Chen* [1995], *Eluszkiewicz* [1996], and *Gettelman et al.* [2000], and estimated from meteorological analyses by *Dethof et al.* [2000].

The fast meridional exchange between tropics and midlatitudes in the lower stratosphere is emphasized in Figure 3a, which shows the seasonal variation of water vapor on the 390 K isentropic level (which is just above the tropical tropopause). At this level the driest air occurs during February-March over 0-20°N, with isolines suggesting transport to NH high latitudes and

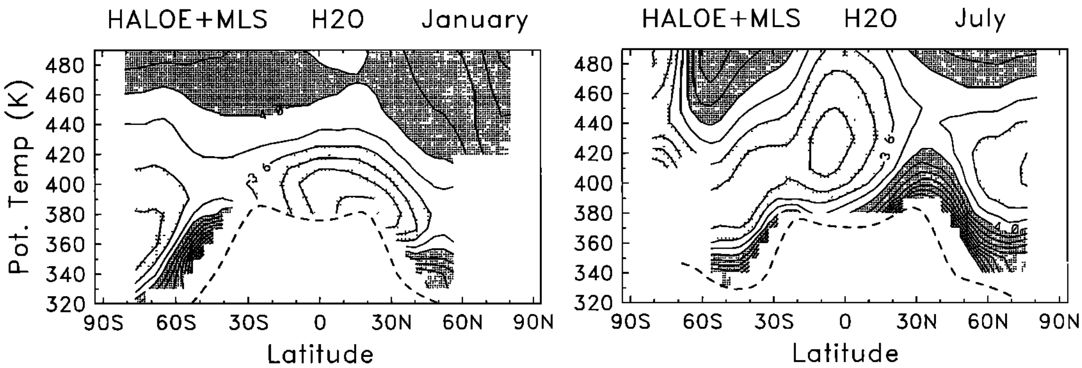

Figure 2. Cross sections of water vapor mixing ratio (ppmv) in (left) January and (right) July, plotted using potential temperature as the vertical coordinate. Dashed lines denote the tropopause.

into the SH with the timescale of ~2 months. A pronounced maximum is observed in NH summer near 30°-40°N, and this appears to be temporally connected with maxima over the equator and SH midlatitudes several months later. While this pattern is suggestive of equatorward transport during NH summer, it may also be a result of separate maxima over 30°-40°N (due to the Asian and North American monsoons [*Jackson et al.* 1998]) and over the tropics due to the seasonal maximum in tropopause temperature during NH summer. As shown below, this tropical maximum during July-October may be biased low in the HALOE retrievals at levels near the tropical tropopause. In any case, the impression for the 390 K level in Figure 3a is one of rapid isentropic meridional exchange over much of the globe. This is in contrast to the situation at 440 K (shown in Figure 3b), where the minimum in water vapor is confined to the tropics, with little inferred transport beyond 30°N-30°S. Comparison of the two levels in Figure 3 demonstrates that the meridional transport occurs primarily in a narrow vertical layer only a few kilometers thick

The amplitude of the water vapor seasonal cycle (over 60°N-60°S) is shown in Figure 4. This is calculated as the maximum minus minimum of monthly values throughout the year, with this amplitude normalized by the respective annual means. This plot emphasizes the large seasonality in the stratosphere below 20 km and shows that the tropical tape recorder signal above 20 km is relatively small in comparison. By far, the largest seasonal cycle is observed in NH midlatitudes in the region near the tropopause, owing primarily to the summer monsoon maximum seen in Figure 3 A comparatively smaller annual cycle occurs in SH midlatitudes The extension of the isolines around the NH maximum in Figure 4 suggests the monsoon influence extends from the deep tropics to polar latitudes.

3.2. Longitudinal Structure

The full three-dimensional variability of water vapor can also be examined using the long record of HALOE data. We find that there is little zonal structure to the HALOE observations above ~18 km (~460 K), but some notable asymmetries in the lowest stratosphere, which provide information on coupling with the troposphere. These asymmetries have been discussed by *Rosenlof et al.* [1997] and *Jackson et al.* [1998]. We briefly discuss these seasonally varying zonal structures based on our longer record, partly as a backdrop for comparisons with the Boulder balloon record (below).

Figure 5 shows the near-global water vapor observations for January at the 390 K isentrope, together with the corresponding 390 K temperature field derived from NCEP reanalysis data. Superimposed on the water vapor plot are heavy contours denoting maxima in climatological convection (specifically, outgoing longwave radiation (OLR) brightness temperatures < 220 K). The water vapor measurements show a minimum over

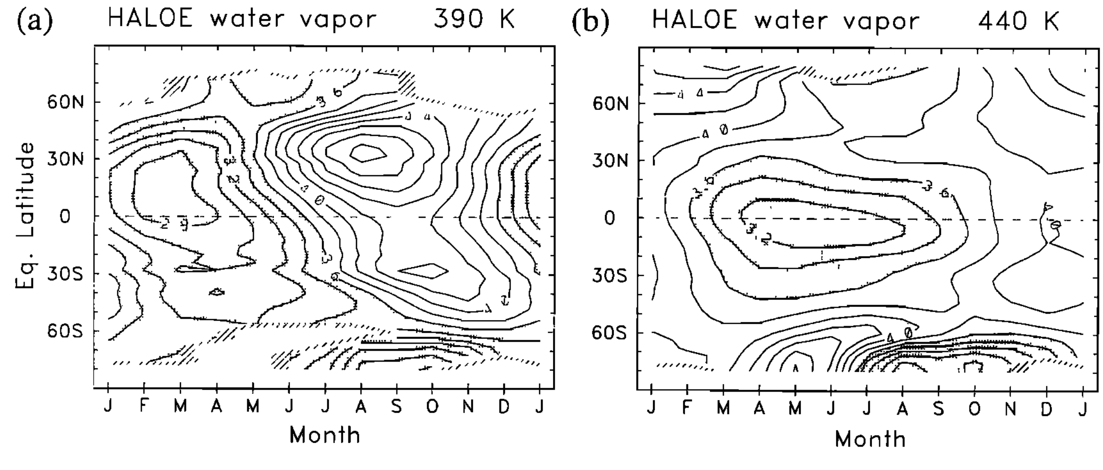

Figure 3. Latitude-time variations of water vapor mixing ratio (ppmv) on potential temperature levels (a) 390 K and (b) 440 K. Data are not available for some months at high latitudes.

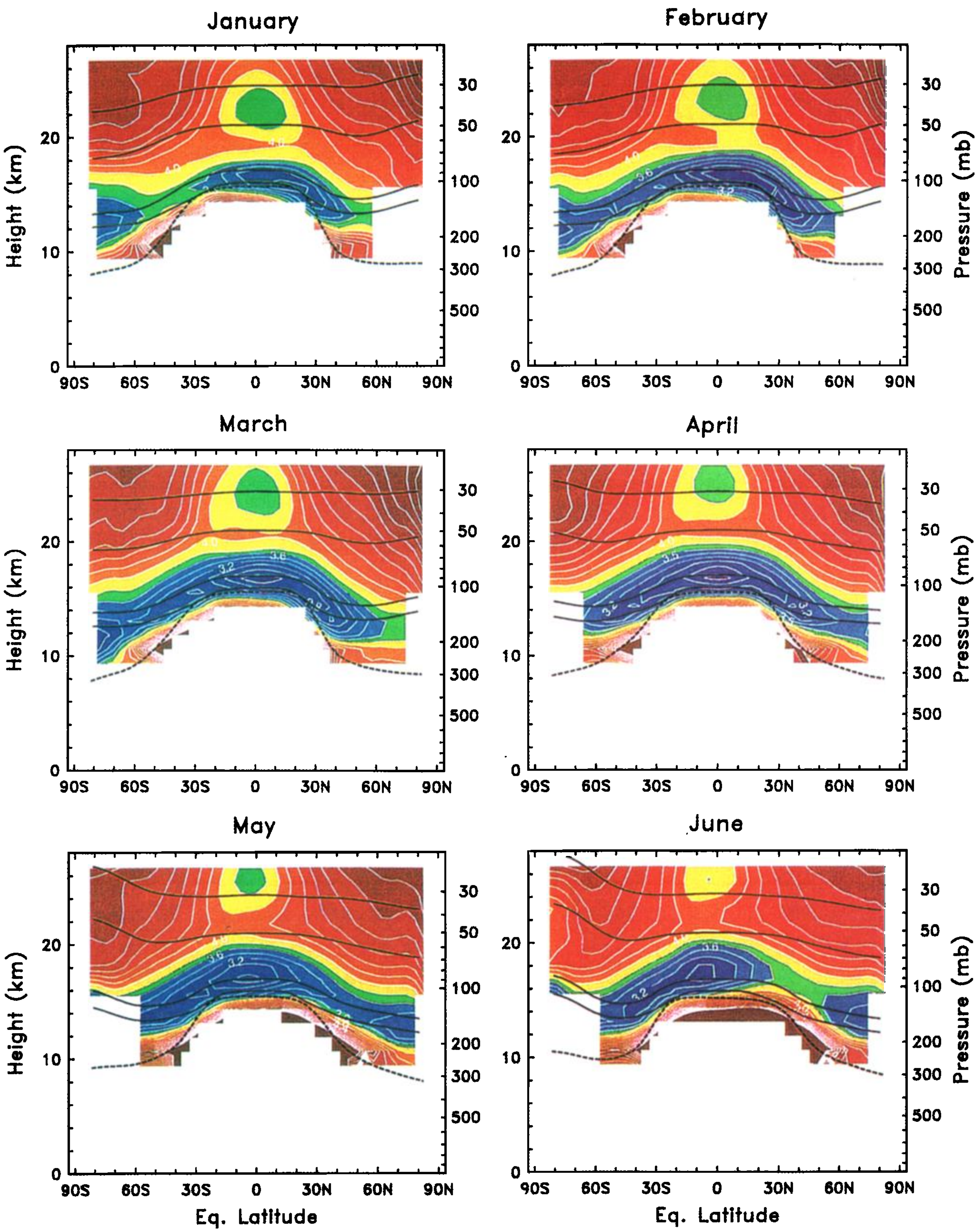

Plate 1. Meridional cross sections of the monthly zonal mean water vapor mixing ratio derived from the Halogen Occultation Experiment (HALOE) plus Microwave Limb Sounder (MLS) climatology. Contour interval is 0.2 ppmv. Dashed lines denote the tropopause, and solid lines denote isentropes of 380, 400, 500 and 600 K (bottom to top).

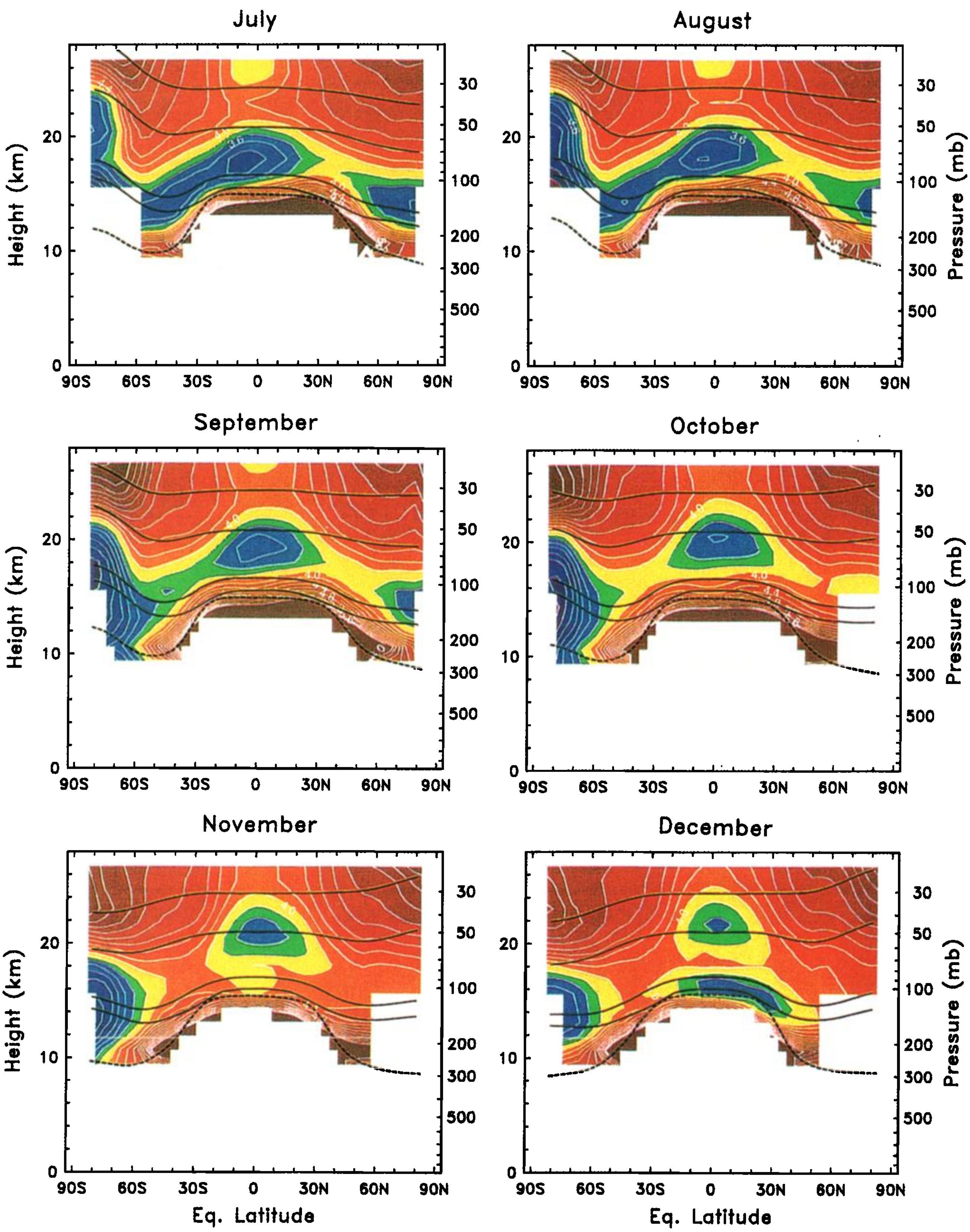

Plate 1. (continued)

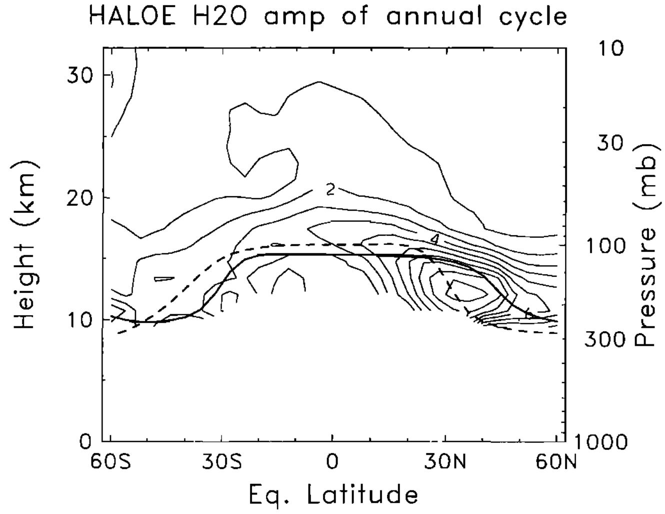

Figure 4. Normalized amplitude of the annual cycle of water vapor mixing ratio derived from HALOE data The amplitude is calculated as the maximum minus minimum during the year, with values normalized by the respective annual mean at each latitude and height Dashed and thick solid lines show the tropopause for January and July, respectively.

~10°S to 25°N, with locally lowest values over the Indonesian region and over Central America. These water vapor minima are correlated (in longitude) with the maxima in convection and the coldest tropical temperatures in both regions However, it is noteworthy that the water vapor minima occur north of the equator (centered near 10°-20°N), whereas the coldest temperatures are centered more nearly on the equator, and maximum convection is somewhat south of the equator (the climatology of tropical convection is discussed by *Waliser and Gautier* [1993])

A height-latitude section of the climatological water vapor structure over the western Pacific region (120°-180°) in January is shown in Figure 6. The minimum values (< 3.0 ppmv) occur near and above the tropopause (dashed line in Figure 6) over ~0 -30°N; the minimum slopes with latitude, approximately following the tropopause and isentropes near 390 K (see Plate 1). Included in Figure 6 are thick contours showing the occurrence frequency of deep tropical convection in the western Pacific, derived from high space-time resolution satellite measurements (A. Gettleman et al., Distribution and effects of convection in the tropical tropopause region, submitted to *Journal of Geophysical Research*, 2001); here the brightness temperature values are used with the background temperature structure to derive the vertical profiles. This figure highlights that the tropospheric convection and coldest tropopause temperatures (shading in Figure 6) are located a substantial distance southward from the driest air in the lower stratosphere Figure 6 also includes the mean meridional (Hadley) circulation in this region (derived from NCEP reanalyses), showing upwelling coincident with convection and strong northward flow across the equator. The sense of this circulation suggests that transport by the local Hadley circulation may be important in understanding the displaced stratospheric water vapor minimum.

Ozone measurements in the lower stratosphere from SAGE II (Figure 7a) show minima in the tropical Indonesian and Central American regions, nearly coincident with the water vapor minima in Figure 5 (with more pronounced minima over Indonesia in both quantities). *Shiotani and Hasebe* [1994] also noted these longitudinal variations in tropical ozone in SAGE II data. The ozone minima are suggestive that this region has had most recent communication with the (low ozone) troposphere. The spatial coincidence with minimum water vapor is consistent with the idealized model of *Sherwood and Dessler* [2001], although the northward displacement with respect to maximum convection (noted above) is not a feature addressed in their study.

The 390 K water vapor and temperature data for July are shown in Figure 8. Relatively high water vapor is observed in NH midlatitudes over ~20°-40°N, with two pronounced maxima over Asia and North America. These maxima are presumably related to enhanced convection and the summer monsoon circulations in these two regions [*Dethoff et al.*, 1999]. While the summer Asian monsoon has a much stronger local circulation

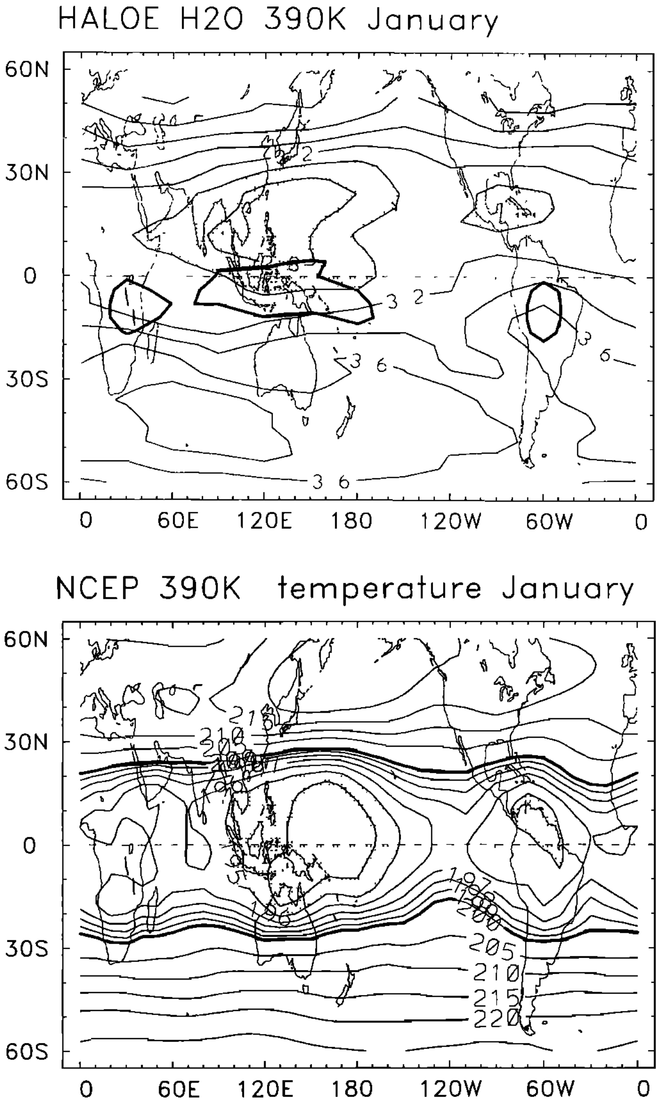

Figure 5. (top) Horizontal structure of water vapor mixing ratio (ppmv) in January at 390 K, with shading denoting relatively dry regions (< 3.0 ppmv). Thick lines denote regions of maximum climatological convection (outgoing longwave radiation (OLR) values below 220 K). (bottom) Temperature at 390 K, derived from National Center for Environmental Prediction (NCEP) reanalysis data

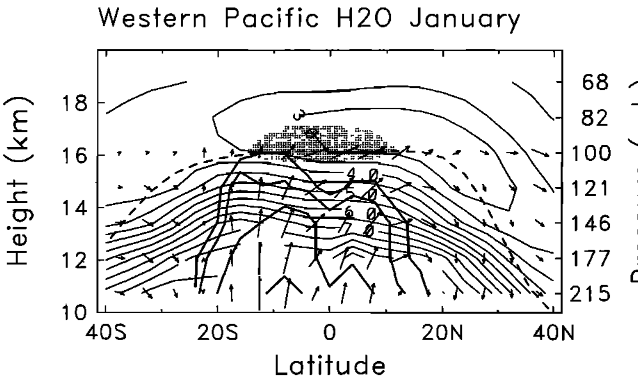

Figure 6. North-south cross section of water vapor, convection, and circulation in the western Pacific in January (all data averaged over 120°-180°E). Thin contours show HALOE water vapor mixing ratios (ppmv). Dashed line is the tropopause, and shading denotes the coldest temperatures near the tropical tropopause (below ~188 K). Thick contours show occurrence frequency of deep tropical convection, based on high-resolution satellite measurements (contours show frequencies of 0.5%, 1%, 3%, and 10%, top to bottom). Vectors show the mean meridional (Hadley) circulation, with the lengths normalized to equivalent displacements over ~1 day.

than that over North America, the HALOE data show nearly equal maxima in water vapor over both regions. A minimum in tropical water vapor is observed over Indonesia in July, coincident with a local minimum in equatorial temperatures. We note that the water vapor minimum is centered south of the equator while maximum July convection is north, and this asymmetry is similar to that observed in January.

Ozone in the lower stratosphere during July (Figure 7b) shows minima in the Asian and North American monsoon regions, approximately coincident with the water vapor maxima. The ozone minimum is much more pronounced over Asia. The ozone maximum over the North Pacific Ocean (between the two minima) may be consistent with enhanced meridional mixing in this region due to the climatological maximum in Rossby wave breaking [*Postel and Hitchman*, 1999]. A distinct ozone minimum is seen in the western Pacific and Indian Ocean region south of the equator, coincident with the tropical water vapor minimum in Figure 8. Again, these low-ozone patterns are indicative of recent communication with the troposphere, and the correlated seasonal variations are evidence of transport into the tropical lower stratosphere throughout the year (and into NH midlatitudes in summer).

3.3. Comparison of HALOE, Aircraft and Balloon Data

The HALOE water vapor data have been found to compare favorably with several independent measurement techniques of *WMO* [2000]. As a complement to that work and to assess the ability of HALOE to sample the seasonal cycle (the focus of this work), we include here comparisons with the tropical seasonal cycle observed in aircraft data and the midlatitudes variations observed by balloon at Boulder, Colorado.

A detailed comparison of the HALOE seasonal variation at the equator with tropical aircraft measurements is shown in Figure 9, for pressure levels 82, 68, and 56 mbar. The HALOE data for each month are shown as a distribution of all tropical (10°N-10°S) measurements during 1992-1999, together with the respective seasonal cycle fits (the same data shown in Figure 1). Included for each pressure level are the aircraft data averaged for each month of observation, together with a curve showing the tropical water vapor seasonal cycle derived by *Andrews et al.* [1999] using empirical age spectra. In Figure 9 we have reduced the aircraft data and the water vapor mixing ratios from the empirical age spectra by 10% to more directly compare seasonal variations, in light of the ~5-20% low bias of HALOE discussed by *WMO* [2000]. Furthermore, the seasonal cycle from MLS water vapor measurements at 68 mbar is included for comparison in Figure 9.

The available aircraft data allow limited sampling of the seasonal cycle with measurements available only from the central Pacific during 7 months spanning 1994-1997. There is substantial variability of these aircraft data about both the HALOE curve and the seasonal cycle predicted by the empirical age spectra (although vertical profiles of the aircraft data agree well with the profiles predicted by the age spectra, as shown by *Andrews et al.* [1999, their Figure 6]). Part of the variability could be attributed to the fact that the aircraft sampling is concentrated in the central Pacific, as compared to the zonal means of HALOE, although the agreement with HALOE is not improved if the HALOE climatology is sampled only in the central Pacific. A large component of variability in the aircraft

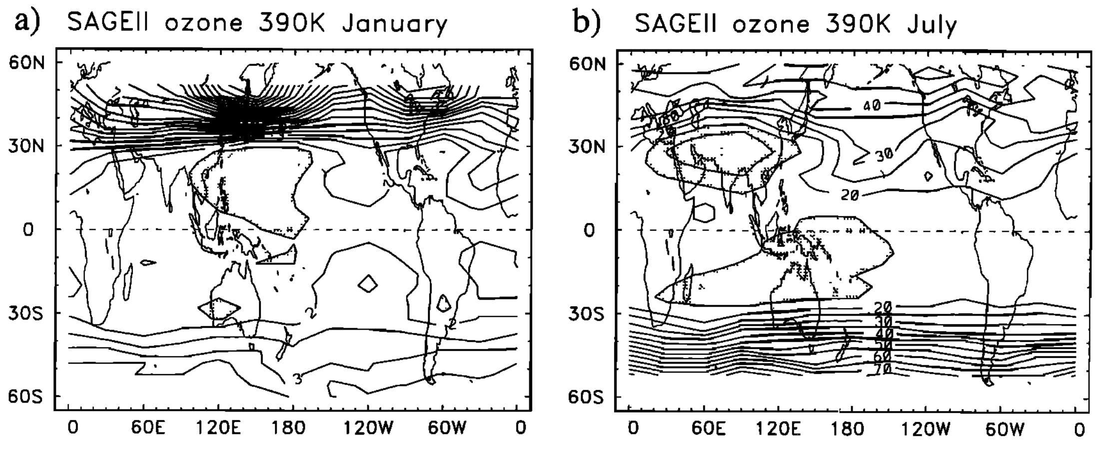

Figure 7. Horizontal structure of ozone mixing ratio (ppmv) at 390 K for (left) January and (right) July, derived from SAGE II data. Shaded regions denote low ozone (< 0.15 ppmv).

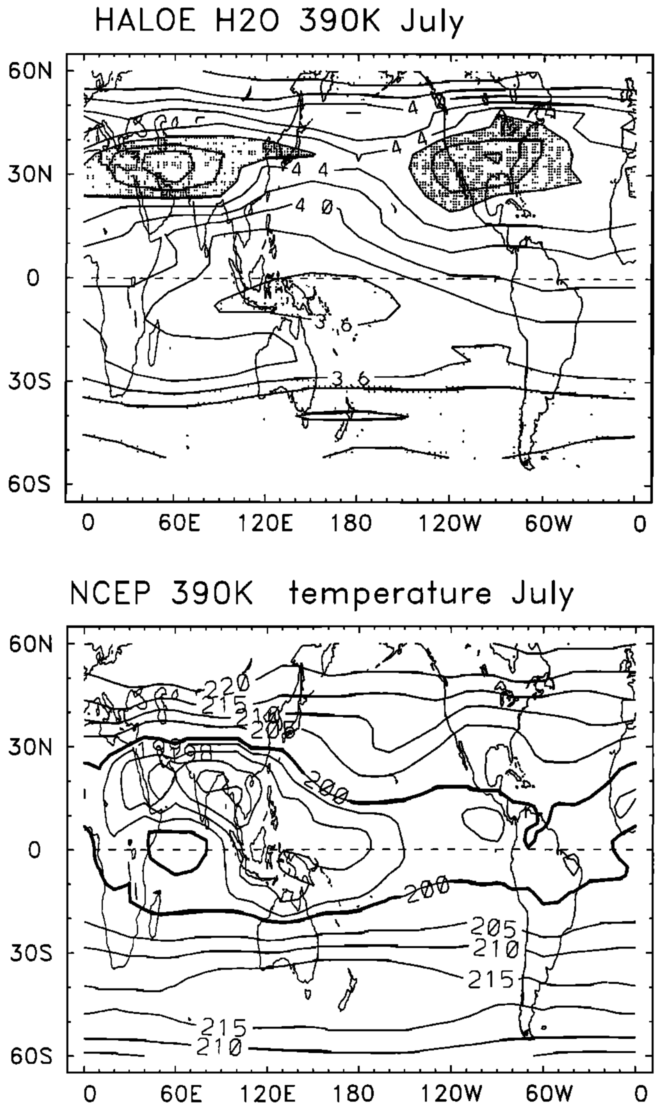

Figure 8. Horizontal structure of (top) water vapor and (bottom) temperature at 390 K in July. Dark and light shading in the top panel denote maxima (> 4 6 ppmv) and minima (< 3.6 ppmv) in water vapor, respectively.

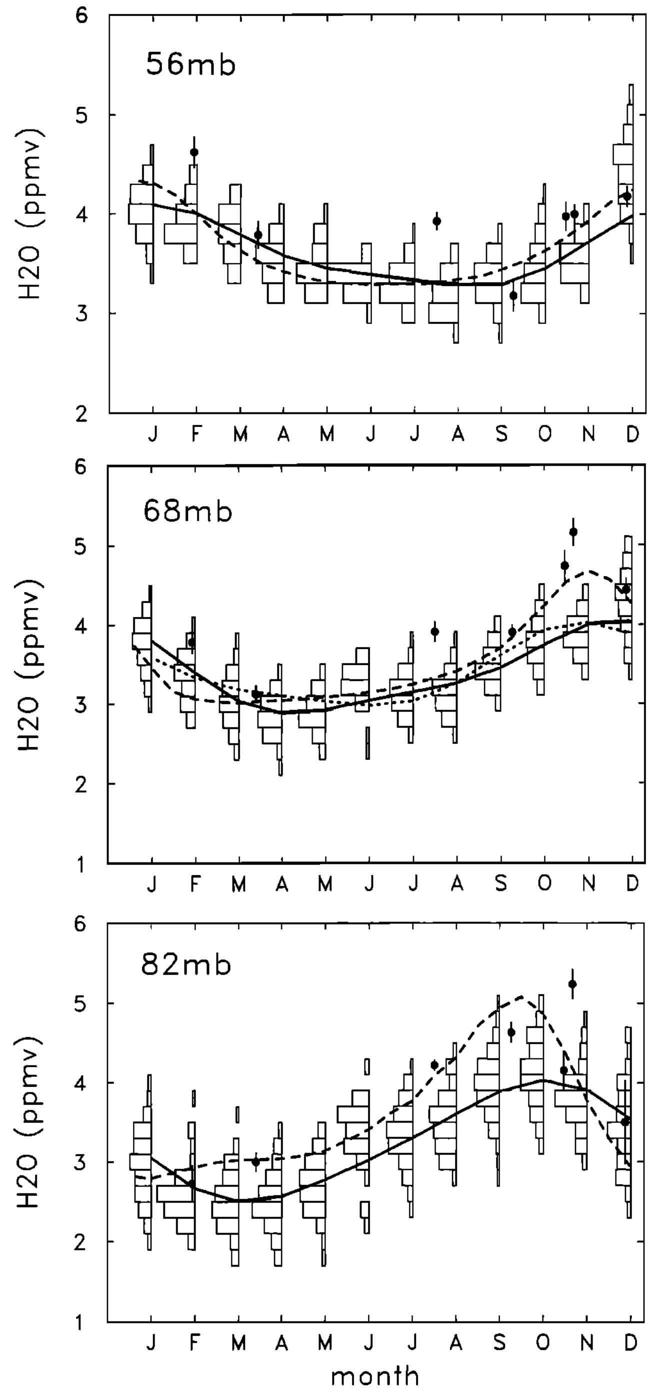

Figure 9. Seasonal variation of water vapor near the equator (10°N-10°S), at 82, 68, and 56 mbar. The histograms for each month show the distribution of all HALOE measurements during 1992-1999, and the thick solid line is the zonal mean seasonal cycle fit Circles denote the means of aircraft measurements from individual field campaigns (discussed in text), with vertical bars showing plus and minus 1 standard deviation of the individual measurements. The dashed line is the water vapor seasonal cycle derived from the empirical age spectra of *Andrews et al.* [1999]. Both the aircraft data and mixing ratios derived from empirical age spectra have been reduced by 10% for more direct comparisons to HALOE (see text). The aircraft and empirical data are archived in potential temperature coordinates and have been interpolated to these pressure levels using a monthly temperature climatology. The dotted line at 68 mbar (only) indicates the seasonal cycle derived from MLS satellite data.

data could also arise from real interannual variability during 1994-1997, which is aliased into the aircraft sampling. A more systematic evaluation of the HALOE tropical data is probably provided by comparisons with the empirical data seasonal cycle. These show good agreement at 56 and 68 mbar, but some notable differences at 82 mbar. At this lower level there is a low bias of HALOE throughout much of the year beyond the 10% accounted for in Figure 9, particularly during August-October. The seasonal cycle is smaller in HALOE than predicted by the empirical age spectra (as noted by *Andrews et al.* [1999]), and the HALOE peak is shifted ~1 month later in time. A similar but smaller systematic difference is seen at 68 mbar near November in Figure 9. A possible cause for these differences is the ~2-km vertical resolution of the HALOE measurements, which can preferentially underestimate the seasonal maximum owing to its narrow vertical scale (as shown by *Mote et al.* [1996], their Figure 1). The seasonal cycle in vertical velocity above the tropical tropopause (which is up to a factor of 2 smaller during July-October; see *Andrews et al* [1999], their Figure 9) will

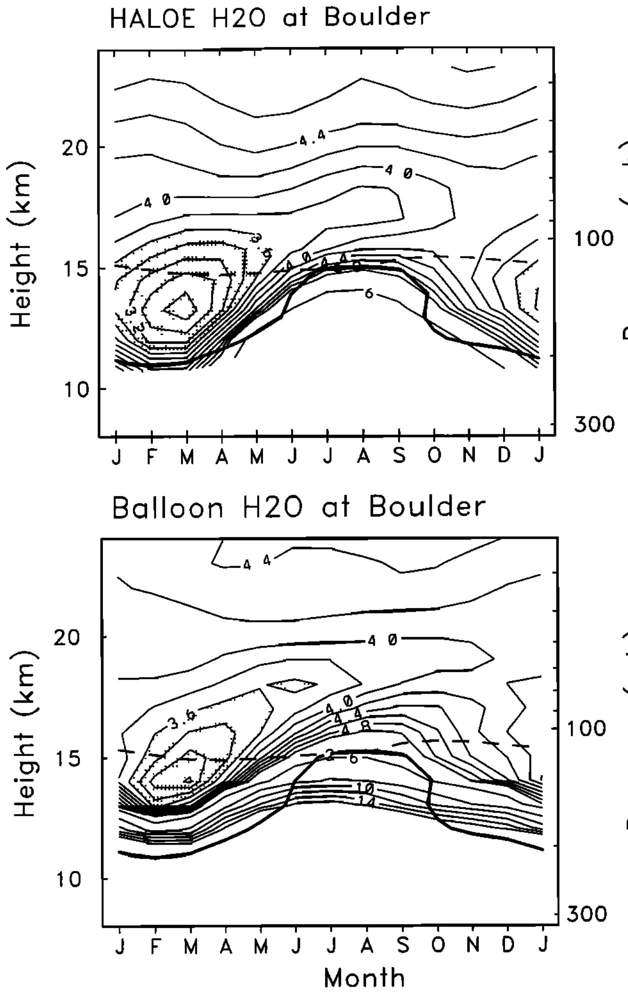

Figure 10. Height-time seasonal variation of water vapor mixing ratio (ppmv) at Boulder, Colorado, derived from (top) HALOE data and (bottom) balloon-borne frost point hygrometer measurements. The thick solid line denotes the tropopause, and the dashed line is the 400 K isentrope.

produce a smaller vertical scale for the tape recorder signal and hence produce preferential biases in HALOE sampling during this time. The overall comparisons are much better at 68 and 56 mbar in Figure 8 (where vertical velocities and tape recorder vertical wavelength are both larger), suggesting the HALOE resolution is less of a problem at these levels (and above).

Height-time sections of the Boulder balloon climatology and HALOE water vapor seasonal cycle interpolated to Boulder (40°N, 105°W) are shown in Figure 10. Overall excellent agreement in the seasonal space-time patterns are found between these independent data. Notably, the location and upward movement of the seasonal minimum from March-August are accurately captured in the HALOE data, and the altitude of the absolute minimum is consistent between the data sets to within 1 km for each month. Direct comparison of the magnitudes shows a (seasonally constant) low HALOE bias of ~7-15% over 121-56 mbar, consistent with the results of *WMO* [2000]. Much more significant HALOE biases are found at lower altitudes during summer at and below the tropopause, where HALOE does not capture the observed high mixing ratios.

The excellent agreement with balloon measurements at Boulder suggests high confidence in the HALOE climatology in the extratropical lower stratosphere. An altitude-time section of HALOE water vapor at a Southern Hemisphere midlatitudes site is shown in Figure 11 for comparison with the Boulder seasonality (the data in Figure 11 are for 40°S, 170°E, near Wellington, New Zealand, but are typical of the entire SH midlatitudes). A minimum in SH midlatitudes water vapor is observed several kilometers above the tropopause during March-April (similar to the NH), due to the rapid transport from the tropics (Figure 3a). Unlike the NH, the altitude of the minimum does not change seasonally in SH midlatitudes, and the overall seasonal variation is much weaker than that in the NH (see Figure 4). This seems mostly attributable to the lack of a strong monsoonal maximum in the SH. While the seasonal minima have similar magnitude between NH and SH, the overall time mean is much larger in the NH, consistent with the aircraft measurements reported by *Kelly et al.* [1990].

4. Summary

The concept of rapid transport between the tropics and midlatitudes in the lower stratosphere has been appreciated for several decades [e.g., *Feely and Spar*, 1960; *Newell*, 1963]. More recent analyses of satellite and aircraft data [*Trepte et al.*, 1993; *Rosenlof et al.*, 1997; *Hintsa et al.*, 1994; *Boering et al.*, 1995] have confirmed this concept based on volcanic aerosol or the seasonally varying signatures of water vapor and carbon dioxide. The high vertical resolution, near-global sampling, and longevity of the HALOE water vapor measurements provide a clear picture of the details of this seasonal transport. Comparisons with the empirical model of tropical water vapor seasonality of *Andrews et al.* [1999] suggest that HALOE accurately measures the seasonal cycle at and above 68 mbar (~19 km). Between the tropopause and 19 km the HALOE data have seasonally varying biases, which cause an underestimate of the seasonal cycle amplitude; these biases may be related to the vertical resolution of HALOE and seasonality in the actual tape recorder vertical structure. Comparisons with the Boulder balloon data show excellent agreement in detail, aside from a ~10% low bias in HALOE V19 retrievals.

The fast seasonal transport in the lower stratosphere occurs near isentropic levels θ ~ 380-420 K; the fact that the water vapor

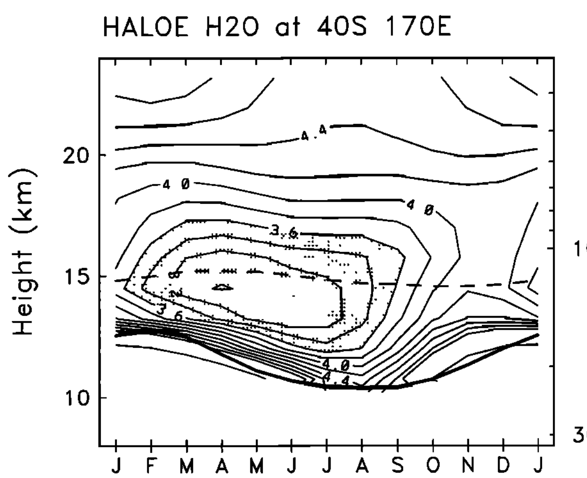

Figure 11. Same as Figure 10, but for seasonal variation of water vapor at midlatitudes in the Southern Hemisphere, derived from HALOE data.

isopleths follow sloping isentropics to midlatitudes is evidence for primarily isentropic transport. Stronger tropical isolation is inferred above θ ~ 440-500 K, so this appears to be the approximate 'base' of the tropical pipe. Although the water vapor data mainly highlight transport into midlatitudes (because the strongest 'signal' originates in the tropics), analyses of other constituent data demonstrate that transport into the tropics is also strong below θ ~ 440 K [*Avalone and Prather*, 1996; *Minschwaner et al*, 1996, *Volk et al*, 1996; *Herman et al.*, 1998; *Flocke et al.*, 1999] While mass continuity suggests that the mean meridional circulation is strongly divergent (poleward flow) in the tropical lower stratosphere [*Rosenlof et al.*, 1997], the two-way constituent transport suggests eddies as a primary transport mechanism. *Chen et al.* [1994] have modeled isentropic transport in this region, showing that eddy transports can effectively mix the tropics and midlatitudes on a ~2 month timescale, consistent with the water vapor observations here. This transport is also modeled in the recent study of *Gettelman et al.* [2000], who simulate the seasonal variation of water vapor in the lower stratosphere based solely on parameterized dehydration and accurate transport.

The NH summer monsoon is a dominant influence on water vapor in the lower stratosphere and, by inference, on other constituents (such as ozone, as seen in Figure 7b). The water vapor data suggest the monsoon is a principal mechanism for transport and tropospheric coupling for the entire NH lower stratosphere. The extent of propagation of moist midlatitudes air into the tropics during approximately August-October is difficult to quantify because of the contemporaneous tropical maximum occurring at this time. Nonetheless, the temporal variations here (Figure 3a) suggest that some fraction of the tropical maximum could be attributable to transport from NH midlatitudes, and this could have an impact on reconciling water vapor with tropical tropopause temperature variations [e.g., *Dessler*, 1998].

The HALOE plus MLS data provide a clear view of the space-time variation of polar dehydration over Antarctica. Temporal development in the data here is consistent with continuous polar measurements by the Polar Ozone and Aerosol Measurement (POAM) instrument [*Nedoluha et al.*, 2000]; strong dehydration begins in July and persists through December. The HALOE data here suggest a remnant of this Antarctic dehydration persists in the lowermost polar stratosphere through summer (well after breakup of the polar vortex). A minimum in water vapor is also observed in the Arctic polar lower stratosphere during summer, although this originates in the tropics rather than developing in situ. This Arctic summer minimum is also observed in POAM observations (G. Nedoluha et al., POAM III measurements of water vapor in the upper troposphere and lowermost stratosphere, submitted to *Journal of Geophysical Research*, 2001). The Arctic water vapor minimum is similar to that in the Antarctic in that it persists throughout the summer. These long-lived isolated minima argue for weak transport through the summer polar stratosphere in both hemispheres, consistent with the polar transport calculations of *Rosenlof* [1999].

Longitudinal variations evident in climatological water vapor (and ozone) data highlight regions of strongest coupling to the troposphere The climatological water vapor data show minima over the Indonesian and Central American regions during NH winter, close to regions of maximum convection and minimum

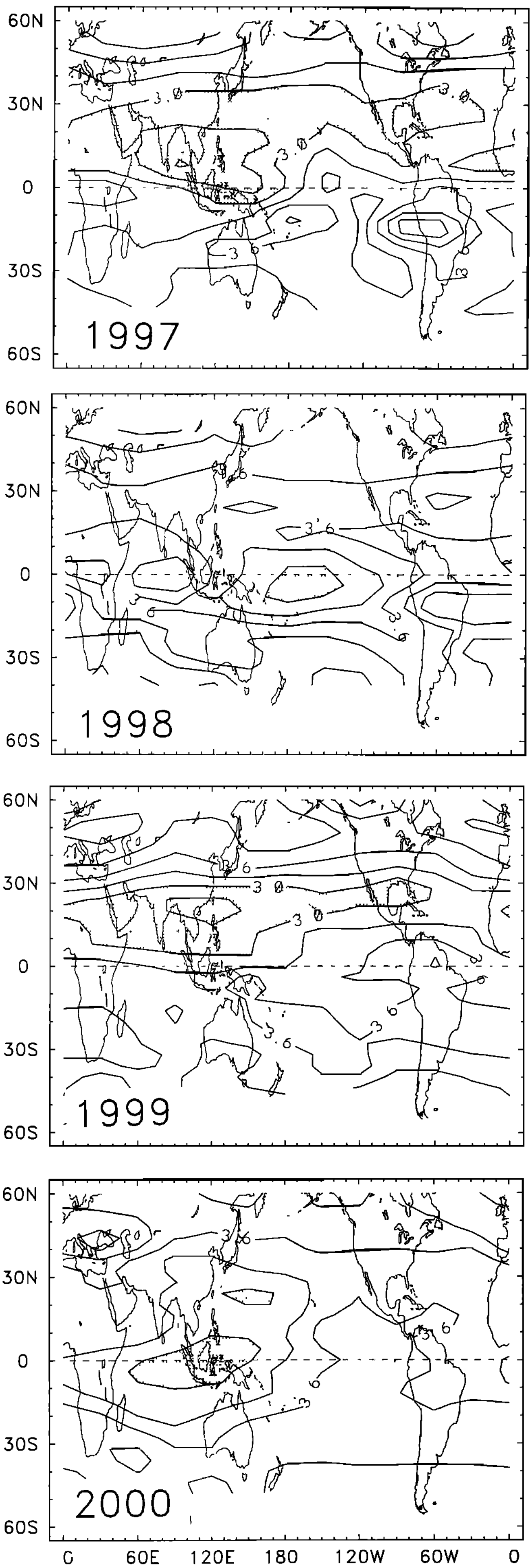

Figure 12. HALOE water vapor mixing ratio on the 390 K isentrope sampled during January-February for the years 1997, 1998, 1999, and 2000. Values below 3 0 ppmv are shaded.

tropopause temperature. There are also coincident minima in ozone in both regions, which are evidence of recent transport from the troposphere. While the patterns (and inferred transport) are strongest over Indonesia, the observed local minima over Central America suggest that air enters the stratosphere over these longitudes also (consistent with the model calculations of *Gettelman et al.* [2000]). An intriguing feature is that the water vapor and ozone minima in January occur north of the equator (centered near 10°-20°N), while minimum temperatures are centered on the equator and convection maximizes slightly south. This is surprising because in the simplest picture one expects minimum water vapor to be colocated with coldest temperatures [e.g., *Newell and Gould-Stewart*, 1981] and possibly with maximum convection [*Danielson*, 1982]. During NH summer, similar spatial patterns and asymmetries are observed in all quantities, with the latitudes reversed (i.e , minimum water vapor and ozone south of the equator). These coherent spatial structures are features that should be reproduced in realistic models of tropical troposphere-stratosphere exchange.

Localized maxima in water vapor are observed in the lower stratosphere over the Asian and North American monsoon regions during NH summer, consistent with direct transport of moist troposphere air into the stratosphere by monsoonal circulations. This hypothesis is consistent with coincident localized minima in ozone. While the ozone and circulation statistics suggest the Asian monsoon to be larger than that over North America, the water vapor data show similarly sized maxima (at least for the relatively short HALOE record). These results confirm the important role of NH monsoonal circulations for constituent budgets in the lower stratosphere on a global scale.

An important detail regarding the climatological variations discussed here is that they are representative of long-term means, and there is significant interannual variability evident in the lower stratosphere. As an example, Figure 12 shows the January-February HALOE water vapor at 390 K for 4 years (1997 through 2000) The years 1997 and 1999 are very similar to the climatology (Figure 5), whereas substantially different patterns are evident in 1998 and 2000. The 1998 year corresponds to a strong El Niño warm event, and the eastward shift of the water vapor minimum to near the date line (Figure 12, 1998) is correlated with a similar eastward shift of tropical convection (these El Niño variations are discussed in detail by *Gettelman et al.* [2001]). El Niño cold event conditions were prevalent during January-February for both 1999 and 2000, although details of the 390 K water vapor are different between these years (the minima are more displaced into the NH for 1999). Overall these figures demonstrate a substantial degree of interannual variability in the HALOE data in the lower stratosphere. While the climatological features in HALOE data are in good overall agreement with seasonality in aircraft and balloon measurements, the utility of HALOE for quantifying interannual variability is a subject of ongoing research

Acknowledgments. The authors thank Elliot Weinstock, Ken Kelly, and Arlyn Andrews for the tropical water vapor data shown in Figure 9 and for their expertise The climatological OLR data were obtained from the NOAA CIRES Climate Diagnostics Center from their web site at http://www.cdc.noaa.gov We thank Rolando Garcia, Jean-Francois Lamarque, and Gerald Nedoluha for discussions and reviews of the text and three anonymous referees for constructive reviews. Marilena Stone expertly prepared the manuscript This work was partially funded by NASA grants W-18181, W-16215, and NAG5-7001 The National Center for Atmospheric Research is sponsored by the National Science Foundation

References

Andrews, A E, et al, Empirical age spectra for the lower tropical stratosphere from in situ observations of CO_2: Implications for stratospheric transport, *J. Geophys. Res.*, *104*, 26,581-26,595, 1999

Avallone, L M., and M J. Prather, Photochemical evolution of ozone in the lower tropical stratosphere, *J. Geophys Res*, *101*, 1457-1461, 1996.

Boering, K A, et al, Measurements of stratospheric carbon dioxide and water vapor at northern midlatitudes: Implications for troposphere-to-stratosphere transport, *Geophys Res Lett.*, *22*, 2737-2740, 1995

Brewer, A W, Evidence for a world circulation provided by measurements of helium and water vapor distribution in the stratosphere, *Q. J. R Meteorol. Soc.*, *75*, 351-363, 1949.

Chen, P., Isentropic cross-tropopause mass exchange in the extratropics, *J. Geophys. Res*, *100*, 16,661-16,673, 1995.

Chen, P., J R Holton, A. O'Neill, and R. Swinbank, Isentropic mass exchange between the tropics and extratropics in the stratosphere, *J Atmos. Sci*, *51*, 3006-3018, 1994

Chiou, E. W., M. P McCormick, and W. P. Chu, Global water vapor distributions in the stratosphere and upper troposphere derived from 5.5 years of SAGE II observations (1986-1991), *J. Geophys. Res.*, *102*, 19,105-19,118, 1997.

Danielson, E F., A dehydration mechanism for the stratosphere, *Geophys Res Lett*, *9*, 605-608, 1982

Dessler, A E., A reexmination of the "stratospheric fountain" hypothesis, *Geophys. Res Lett.*, *25*, 4165-4168, 1998

Dethof, A., A. O'Neill, J. M Slingo, and H. A Smit, A mechanism for moistening the lower stratosphere involving the Asian summer monsoon, *Q J R Meteorol. Soc*, *125*, 1079-1106, 1999.

Dethof, A., A. O'Neill, and J Slingo, Quantification of the isentropic mass transport across the dynamical tropopause, *J. Geophys Res*, *105*, 12,279-12,293, 2000

Eluszkiewicz, J, A three-dimensional view of the stratosphere-to-troposphere exchange in the GFDL SKYHI model, *Geophys. Res. Lett.*, *23*, 2489-2492, 1996

Feely, H W, and J. Spar, Tungsten-185 from nuclear bomb tests as a tracer for stratospheric meteorology, *Nature, 188,* 1062-1064, 1960

Flocke, F, et al., An examination of chemistry and transport process in the tropical lower stratosphere using observations of long-lived and short-lived compounds obtained during STRAT and POLARIS, *J. Geophys Res*, *104*, 26,625-26,642, 1999

Gettelman, A, J R. Holton, and A R Douglass, Simulations of water vapor in the lower stratosphere and upper troposphere, *J Geophys. Res*, *105*, 9003-9023, 2000.

Gettelman, A, W J Randel, S. Massie, F Wu, W. Read, and J. M Russell III, El-Nino as a natural experiment for studying the tropical tropopause region, *J Clim*, in press, 2001

Hall, T M, and D W Waugh, Tracer transport in the tropical stratosphere due to vertical diffusion and horizontal mixing, *Geophys. Res. Lett.*, *24*, 1383-1386, 1997

Harries, J E., S Ruth, and J M Russell III, Validation of measurements of water vapor from the Halogen Occultation Experiment, *J Geophys Res.*, *101*, 10,205-10,216, 1996.

Herman, R L, et al., Tropical entrainment timescales inferred from stratospheric N_2O and CH_4 observations, *Geophys Res Lett.*, *25*, 2781-2784, 1998

Hintsa, E. J., et al, SPADE H2O measurements and the seasonal cycle of stratospheric water vapor, *Geophys. Res. Lett*, *21*, 2559-2562, 1994.

Hintsa, E. J, E M Weinstock, J. G Anderson, R. D. May, and D F Hurst, On the accuracy of in situ water vapor measurements in the troposphere and lower stratosphere with the Harvard Lyman-α hygrometer, *J Geophys. Res.*, *104*, 8183-8189, 1999

Hitchman, M H, M McKay, and C. R Trepte, A climatology of stratospheric aerosol, *J. Geophys. Res.*, *99*, 20,689-20,700, 1994

Hyson, P, Stratospheric water vapor over Australia, *Q J. R. Meteorol. Soc*, *109*, 285-294, 1983

Jackson, D R, S J Driscoll, E J. Highwood, J. E. Harries, and J M Russell III, Troposphere to stratosphere transport at low latitudes as studied using HALOE observations of water vapor 1992-1997, *Q. J R Meteorol. Soc.*, *124*, 169-192, 1998

Kalnay, E, et al, The NCEP/NCAR 40-year reanalysis project, *Bull Am Meteorol. Soc.*, *77*, 437-471, 1996

Kelly, K K., A F. Tuck, L E Heidt, M. Loewenstein, J F Podolske, and S. E Strahan, A comparison of ER-2 measurements of stratospheric water vapor between the 1987 Antarctic and 1989 Arctic airborne missions, *Geophys. Res. Lett*, *17*, 465-468, 1990

Kley, D, A. Schmeltekopf, K. Kelly, R Winkler, T Thompson, and M

McFarland, The U-2 Lyman-Alpha results from the 1980 Panama Experiment, in *The Stratospheric-Tropospheric Exchange Experiment*, edited by A P Margozzi, *NASA Tech. Memo, 84297,* 82-125, 1983

Mastenbrook, H J., Water vapor measurements in the lower stratosphere, *Can. J Chem*, *52*, 1527-1531, 1974

Mastenbrook, H J, and S J Oltmans, Stratospheric water vapor variability for Washington, D C./Boulder, Colorado: 1964-82, *J Atmos Sci*, *40*, 2157-2165, 1983

McCormick, M P, J M Zawodny, R E Viega, J C Larsen, and P H Wang, An overview of SAGE I and II ozone measurements, *Planet Space Sci*, *37*, 1567-1586, 1989

McCormick, M. P, et al, Annual variations of water vapor in the stratosphere and upper troposphere observed by the Stratospheric Aerosol and Gas Experiment II, *J Geophys. Res*, *98*, 4867-4874, 1993

Michelson, H A., F W Irion, G L Manney, G C Toon, and M R Gunson, Features and trends in Atmospheric Trace Molecule Spectroscopy (ATMOS) version 3 stratospheric water vapor and methane measurements, *J Geophys. Res.*, *105*, 22,713-22,714, 2000

Minschwaner, K, A E Dessler, J W Elkins, C M Volk, D W Fahey, M Loewenstein, J. R Podolske, A E Roche, and K R Chan, The bulk properties of isentropic mixing into the tropics in the lower stratosphere, *J. Geophys. Res.*, *101*, 9433-9439, 1996.

Mote, P W, K. H Rosenlof, J R. Holton, R S. Harwood, and J W. Waters, An atmospheric tape recorder The imprint of tropical tropopause temperatures on stratospheric water vapor, *J Geophys Res.*, *101*, 3989-4006, 1996

Mote, P. W., T J Dunkerton, M E McIntyre, E. A Ray, P H Haynes, and J M. Russell III, Vertical velocity, vertical diffusion, and dilution by midlatitude air in the tropical lower stratosphere, *J Geophys Res*, *103*, 8651-8666, 1998

Nedoluha, G. E., et al., POAM III measurements of dehydration in the Antarctic lower stratosphere, *Geophys Res Lett*, *27*, 1683-1686, 2000.

Newell, R. E, Transfer through the tropopause and within the stratosphere, *Q J R Meteorol Soc*, *89*, 167-203, 1963

Newell, R. E, and S. Gould-Stewart, A stratospheric fountain?, *J. Atmos Sci.*, *38*, 2789-2796, 1981

Oltmans, S J, H Volmel, D J Hofmann, K Rosenlof, and D Kley, The increase in stratospheric water vapor from balloon borne frostpoint hygrometer measurements at Washington, D C and Boulder, Colorado, *Geophys Res Lett*, *27*, 3453-3456, 2000

Pan, L, S. Solomon, W Randel, J -F Lamarque, P. Hess, J Gille, E -W Chiou, and M P McCormick, Hemispheric asymmetries and seasonal variations of the lowermost stratospheric water vapor and ozone derived from SAGE II data, *J Geophys Res*, *102*, 28,177-28,184, 1997

Pan, L L, E J, Hintsa, E M Stone, E M. Weinstock, and W J Randel, The seasonal cycle of water vapor and saturation vapor mixing ratio in the extratropical lowermost stratosphere, *J Geophys Res*, *105*, 26,519-26,530, 2000

Pierce, R. B, W. Grose, J R Russell III, A F Tuck, R Swinbank, and A O'Neill, Spring dehydration in the Antarctic stratosphere vortex observed by HALOE, *J Atmos Sci*, *51*, 2931-2941, 1994

Postel, G A, and M H Hitchman, A climatology of Rossby wave breaking along the subtropical tropopause, *J Atmos Sci.*, *56*, 359-373, 1999

Pumphrey, H C, Validation of a new prototype water vapor retrieval for UARS MLS, *J Geophys. Res*, *104*, 9399-9412, 1999.

Pumphrey, H. C., H. L. Clark, and R. S Harwood, Lower stratospheric water vapor measured by UARS MLS, *Geophys. Res. Lett*, *27*, 1691-1694, 2000.

Randel, W J, F Wu, J. M Russell III, A Roche, and J W Waters, Seasonal cycles and QBO variations in stratospheric CH_4 and H_2O observed in *UARS* HALOE data, *J Atmos Sci*, *55*, 163-185, 1998

Rosenlof, K H, Estimates of the seasonal cycle of mass and ozone transport at high northern latitudes, *J Geophys Res*, *104*, 26,511-26,523, 1999

Rosenlof, K H, A F Tuck, K K Kelly, J M Russell III, and M. P McCormick, Hemispheric asymmetries in water vapor and inferences about transport in the lower stratosphere, *J Geophys Res*, *102*, 13,213-13,234, 1997

Russell, J M, III, A F Tuck, L L Gordley, J H Park, S R Drayson, J E Harries, R J Cicerone, and P J Crutzen, The HALOGEN Occultation Experiment, *J Geophys Res*, *98*, 10,777-10,797, 1993.

Sherwood, S C, and A E Dessler, A model for transport across the tropical tropopause, *J Atmos Sci.*, *58*, 765-779, 2001

Shiotani, M, and F. Hasebe, Stratospheric ozone variations in the equatorial region as seen in Stratospheric Aerosol and Gas Experiment data, *J Geophys Res*, 99, 14,575-14,584, 1994

Strahan, S E, A R Douglass, J E. Nielsen, and K A Boering, The CO_2 seasonal cycle as a tracer of transport, *J Geophys Res*, *103*, 13,729-13,741, 1998.

Trepte, C, and M Hitchman, Tropical stratospheric circulation deduced from satellite aersol data, *Nature, 355*, 626-628, 1992

Trepte, C R., R E. Veiga, and M. P McCormick, The poleward dispersal of the Mt Pinatubo volcanic aerosol, *J Geophys Res*, *98*, 18,562-18,573, 1993

Tuck, A F, J M Russell III, and J. E Harries, Stratospheric dryness: Antiphased dessication over Micronesia and Antarctica, *Geophys Res. Lett.*, *20*, 1227-1230, 1993.

Volk, C M, et al., Quantifying transport between the tropical and midlatitudes lower stratosphere, *Science*, *272*, 1763-1768, 1996.

Waliser, D E, and C Gautier, A global climatology of the ITCZ, *J. Clim.*, *6*, 2162-2174, 1993

Weinstock, E M., E J. Hintsa, A E. Dessler, J. F Oliver, N L Hazen, J N. Demusz, N T Allen, L B. Lapson, and J G Anderson, A new fast-response photofragment fluorescence hygrometer for use on the ER-2 and Perseus remotely piloted aircraft, *Rev Sci Instrum*, *65*, 3544-3554, 1994

World Meteorological Organization, Stratospheric processes and their role in climate (SPARC) assessment of upper tropospheric and stratospheric water vapour, *SPARC Rep 2, WCRP-113, WMO/TD-1043*, Geneva, 2000

A Gettelman, W J Randel, and F Wu, National Center for Atmospheric Research, 1850 Table Mesa Drive, Boulder, CO 80305 (randel@ucar edu)

S J Oltmans, NOAA Climate Monitoring and Diagnostics Laboratory, Boulder, CO 80305.

J. M. Russell III, Center for Atmospheric Sciences, Hampton University, Hampton, VA 23668

J M Zawodny, NASA Langley Research Center, Hampton, VA

(Received August 15, 2000; revised December 11, 2000, accepted January 8, 2001)